Viscoelastic Fluid Description of Bacterial Biofilm Material Properties

I. Klapper,[1] C. J. Rupp,[2] R. Cargo,[2] B. Purvedorj,[2] P. Stoodley[2,3]

[1]Department of Mathematical Sciences, Montana State University, Bozeman, MT 59717; telephone: (406) 994-5231; fax: (406) 994-1789; e-mail: klapper@math.montana.edu
[2]Center for Biofilm Engineering, Montana State University, Bozeman, Montana 59717
[3]Departments of Microbiology and Civil Engineering, Montana State University, Bozeman, Montana 59717

Abstract: A mathematical model describing the constitutive properties of biofilms is required for predicting biofilm deformation, failure, and detachment in response to mechanical forces. Laboratory observations indicate that biofilms are viscoelastic materials. Likewise, current knowledge of biofilm internal structure suggests modeling biofilms as associated polymer viscoelastic systems. Supporting experimental results and a system of viscoelastic fluid equations with a linear Jeffreys viscoelastic stress–strain law are presented here. This system of equations is based on elements of associated polymer physics and is also consistent with presented and previous experimental results. A number of predictions can be made. One particularly interesting result is the prediction of an elastic relaxation time on the order of a few minutes—biofilm disturbances on shorter time scales produce an elastic response, biofilm disturbances on longer time scales result in viscous flow, i.e., nonreversible biofilm deformation. Although not previously recognized, evidence of this phenomenon is in fact present in recent experimental results. © 2002 Wiley Periodicals, Inc. Biotechnol Bioeng 80: 289–296, 2002.
Keywords: biofilm; mechanical properties; shear stress; strength; viscoelasticity

INTRODUCTION

Bacterial biofilms accumulate on virtually all wetted surfaces and are a recognized problem in industrial pipelines, where they are associated with increased pressure drop, product contamination, and corrosion. Moreover, detachment from biofilms in food production facilities and drinking water systems may result in the potential transmission of pathogens via contaminated food (Piriou et al., 1997), drinking water (Walker et al., 1995), or aerosols (Zottola and Sasahara, 1994).

Biofilm bacteria commonly produce an extracellular polymeric slime (EPS) matrix that protects them against antimicrobial agents and desiccation and also provides mechanical stability to the biofilm (Flemming et al., 2000). However, little is known about the material properties or adhesive and cohesive strengths of attached biofilms, making it difficult to predict how a biofilm may behave in response to an applied force. In a flowing system the fluid will exert a shear stress on the biofilm and colliding particulates may exert both normal and shear stresses.

In earlier work we developed a microscopic method in which the deformation of individual biofilm cell clusters was related to the fluid shear stress to conduct in situ tests analogous to stress–strain and creep tests (Stoodley et al., 1999a, 2001a). Data from these experiments and viscosity measurements on detached biofilms by Ohashi and Harada (1994) suggest that both mixed species and pure culture biofilms behaved like viscoelastic fluids—biofilms exhibit both irreversible viscous deformation and reversible elastic response and recoil. These experiments show biofilms reacting to stress both as an elastic solid and a viscous fluid. Furthermore, the nature of those reactions apparently depends in part on the biofilm history; in particular, its stress history.

Stress response is also recognized to be relevant to biofilm modeling. For the most part, however, biofilm models have not included biofilm material properties (Gujer and Wanner, 1990; Hermanowicz, 1998; Dockery and Klapper, 2001), although some authors have recognized the importance of this issue. Picioreanu et al. (2001), in a study of detachment in biofilm processes, constructed a model in which the biofilm has a partial elastic response to fluid stress—once local internal stresses exceed a cohesive strength the biofilm detaches and the model predicts detachment of discrete cell clusters from the biofilm. Fluid stress has also been considered in microscale biofilm simulations (Dillon et al., 1996).

We suggest that development of a robust, versatile theory of biofilm stress response is essential for understanding and prediction of biofilm structural stability. In this article we propose a description of biofilms as viscoelastic fluids. The conceptual basis of this description is a model developed to describe reversible networks and associated polymeric systems (Leiber et al., 1991; Rubinstein and Dobrynin, 1997) justified by experimental data interpretable in terms of the various chemical and physical interactions between the biofilm matrix polymers. The conceptual and mathematical models proposed here are based on the assumption that biofilms can be viewed as associated polymer networks. The viscoelastic component of this model will allow interrogation of time-dependent deformation in response to shear over different time scales. Such a model can also accommodate the apparent fluid-like behavior of biofilm ripples (regularly spaced surface waves) moving downstream across solid surfaces in response to shear stress from the bulk fluid flow (Stoodley et al., 1999b) and provide natural mechanical explanations for a number of other observed biofilm phenomena, e.g., density increase under shear stress (Vieira et al., 1993) and oscillation of biofilm streamers (Stoodley et al., 1998, 1999a).

In this article we present data from high and low transient shear tests on biofilms grown from various strains of *Pseudomonas aeruginosa* from published and previously unpublished experiments. These data and other data from the literature motivate our proposed viscoelastic constitutive model. There are two main thrusts of this study: first, using previous data in addition to new data, we wish to argue that biofilms should be regarded constitutively as viscoelastic fluids. Second, we propose a viscoelastic fluid model which can explain a number of biofilm material phenomena in a straightforward manner. A third part of this article attempts estimation of parameter values from available data. Those data are insufficient to prove or disprove the model validity. Instead, our aim is to check that the available data is consistent with the model and to construct best current estimates of material parameter values.

MATERIALS AND METHODS

Bacterial Strains and Biofilm Growth Conditions

Biofilms were grown from three strains of *Pseudomonas aeruginosa* in square glass flow cells ($0.3 \times 0.3 \times 20$ cm length) under steady laminar and turbulent flows with a range of wall shear stresses from 0.005 N/m^2 to 5.3 N/m^2. Table I shows the strains used and the growth conditions for the various experiments. For the low shear experiments the flow cells were positioned in a "once-through system" in which sterile nutrients were pumped at a constant flow velocity through the flow cells. The flow cells were inoculated by injecting 1 ml of a 24-h shake broth culture through an injection port which was positioned immediately upstream of the flow cells. A period of 1 h was allowed for attachment before the nutrient flow was initiated. For the high shear experiments the flow cells were positioned in a recirculating loop attached to a mixing chamber. Sterile nutrients were continually added to the mixing chamber, which had a waste overflow (Stoodley et al., 1999a). The flow velocity was continuously monitored using either flow meters (McMillan Flo-sensor; Cole-Parmer, Niles, IL) or volumetric flow rate. The fluid shear stress at the wall (τ_w) was calculated from the average flow velocity as described elsewhere (Stoodley et al., 1999a). The specific wall shear stress at which each biofilm was grown is denoted τ_{wg}. The system was inoculated by injecting 1 ml of thawed stock culture into the mixing chamber and was operated in batch mode for 24 h before switching to continuous culture by switching on the nutrients supply. There was recirculating flow through the flow cells during the inoculation phase. The hydraulic residence time in both systems was kept below the doubling time, which ranged from 1.20 ± 0.19 h for

Table I. Bacterial strains and growth conditions.

Strain	Reference	Relevant genotype or phenotype	Growth medium	Growth system and growth wall shear stress (τ_{wg})
PAO1	Holloway et al. (1979)	Prototrophic, nonmucoid opportunistic pathogen	Minimal salts medium (MSM) with 400 ppm glucose (Stoodley et al., 1999a)	Recirculating, 5.1 N/m^2
PAO1	Holloway et al. (1979)	Protrophic, nonmucoid opportunistic pathogen	1/50 strength Leuria broth	Recirculating, 0.09 N/m^2 and 5.3 N/m^2
PAO-JP1	Pearson et al. (1997)	$\Delta lasI$:tet, LasI mutant derived from PAO1. Does not produce the quorum sensing signal N-3-oxo-dodecanoyl homoserine lactone	1/50 Leuria broth	Once through, 0.005 N/m^2
FRD1	Nivens et al. (2001)	Mucoid cystic fibrosis isolate	Minimal salts medium with sodium glutamate (13 mg/l)	Once through, 0.007 N/m^2

PAO1 to 3.14 ± 0.14 h for FRD1 to minimize planktonic growth. The biofilms were grown between 7 and 10 days at 25°C. The flow cells were positioned on the stage of an Olympus BH2 microscope for in situ microscopic examination. Digital time-lapse images were captured with a COHU 4612-5000 CCD camera (Cohu, San Diego, CA) and a Scion VG-5 PCI framestore board (Scion, Frederick, MD). Images were analyzed using Scion Image (http://rsb.info.gov/nih-image/).

Stress–Strain Curves

Stress–strain curves of individual cell clusters were generated by measuring the length of individual cell clusters at different fluid shear stresses. The strain was calculated by dividing the change in cell cluster length (in response to a change in fluid shear) by the original length. Each incremental measurement took approximately 10 sec, during which time the flow rate was increased and an image captured on the computer. In this study the length at τ_{wg} was taken as the original length so that a positive strain represents an elongation and a negative strain a contraction. For PAO1, initially the stress–strain relationship was measured between τ_w of 0–5.7 N/m^2 (loading portion of the test) and then decrementally back to 0 N/m^2 (unloading portion). The complete test took approximately 180 sec to perform. A repeat loading test was then performed but in this case τ_w was incrementally raised to 17.6 N/m^2 and back to 0 N/m^2 over 210 sec. A similar test was performed on the FRD1 biofilm. Initially, τ_w was raised incrementally to 0.34 N/m^2 over a 90-sec period before decrementally returning to 0 N/m^2. A repeat loading test was performed, increasing τ_w to 47 N/m^2. An apparent elastic modulus (G) was estimated using linear regression analysis of the linear region of the loading portion of the curves according to $G = \tau_w/\epsilon$, where ϵ was the measured strain.

RESULTS AND DISCUSSION

Experimental Results

After 10 days the PAO1 biofilm consisted of filamentous streamers that were elongated in the downstream direction (Fig. 1). The stress–strain test was performed at this time. For the low shear test (Fig. 2a) the stress–strain curve was linear in both loading and unloading with no discernable hysteresis. This curve was characteristic of an elastic response. However, when τ_w was increased to 17.6 N/m^2, over three times that of τ_{wg}, there was a measurable hysteresis between the loading and unloading curves, demonstrating both a viscous and an elastic response (Fig. 2b). G was approximately 115 N/m^2 ($r^2 = 1.00$, n = 15), a similar value to that reported in previous experiments for mixed species biofilms grown under the same shear stress of 5.1 N/m^2
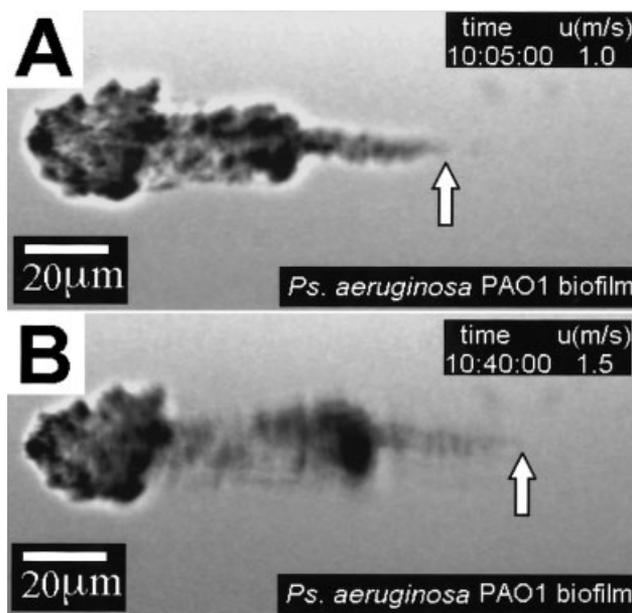

Figure 1. Elongation of biofilm in response to elevated shear stress. The PAO1 biofilm was grown for 7 days under turbulent flow at a velocity of 1 m/s (Re = 3,600, τ_{wg} = 5.1 N/m^2). The biofilm developed filamentous streamers which were attached to the substratum by an upstream "head" while the "tails" were free to oscillate in the flow (top panel). When the velocity was increased to 1.5 m/s (τ_{wg} = 10.4 N/m^2) the streamer elongated elastically and acquired an immediate elastic strain of 0.03, indicating a value of G of 162 N/m^2. The biofilm then demonstrated viscous creep over time so that after 4 min it had accumulated a strain of approximately 0.20 (bottom panel). Arrows point to the streamer tips. A video sequence "Shear induced creep and detachment of *Pseudomonas aeruginosa* PAO1 biofilm streamer" showing the biofilm elongation in response to elevated fluid shear has been posted at the site http://www.erc.montana.edu/res-Lib99-sw/movies.

(Stoodley et al., 1999a). The FRD1 biofilm that was grown under laminar flow consisted of hemispherical-shaped cell clusters. For the low shear test the stress–strain curve was nonlinear (Fig. 3a). Between τ_w of 0.04 and 0.18 N/m^2 there was a linear region with a corresponding G of 6.3 N/m^2 ($r^2 = 0.97$, n = 4). Between τ_w of 0.18 and 0.26 N/m^2 there was a plateau region. Above $\tau_w = 0.26$ N/m^2 the biofilm cluster became stiffer, possibly due to polymer alignment and the extrusion of water, which can act as a plasticizer in biological tissues (Vincent, 1990). The hysteresis between the loading and unloading portions of the curve demonstrated a viscous response and the residual strain indicated that the biofilm had flowed during the test. The high shear test (Fig. 3b) gave a J-shaped curve characteristic of aligned polymer biological systems such as collagen and rubber (Vincent, 1990). The linear low modulus region gave a G of 71 N/m^2 ($r^2 = 0.92$, n = 8). Table II contains experimentally observed values of G for the various *Pseudomonas* strains, together with the values of τ_{wg}. Although these data were compiled from experiments using different strains and growth conditions, they would appear to indicate G increases with increasing
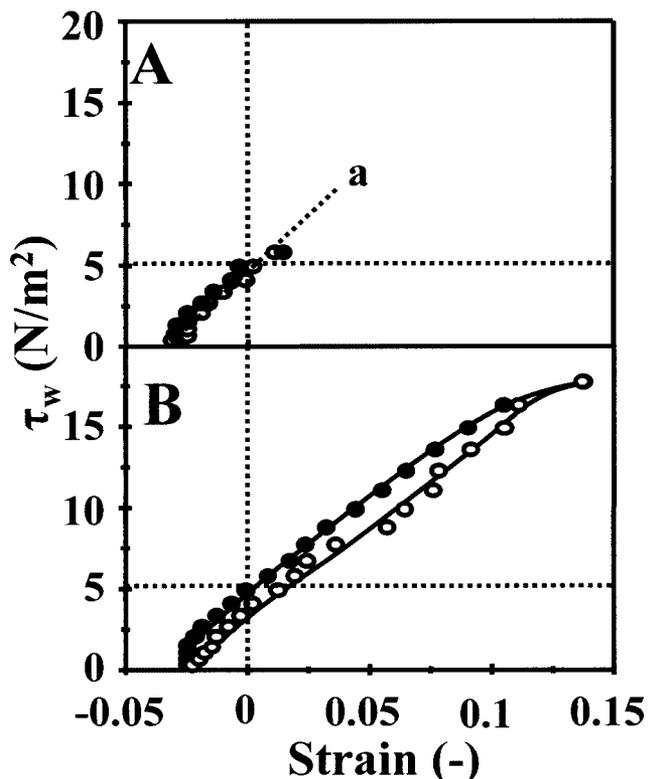
Figure 2. Stress–strain curves for *Pseudomonas aeruginosa* PAO1. The biofilm was grown at a flow velocity of 1 m/s with a corresponding wall shear stress of 5.1 N/m² (horizontal line). A: Low shear test indicates a linear elastic response with no discernable hysteresis. B: Hysteresis in high shear test demonstrates a viscoelastic lag response. Closed symbols correspond to the loading cycle and the open symbols to the unloading cycle. The biofilm contracted (negative strain) when the fluid shear was dropped below the growth shear, indicating that under growth shear the biofilm matrix had developed a stress loading. Individual measurements were made in 10-sec intervals.

τ_{wg}. Pending further data we will approximate the relation between the two quantities as linear in the model presented below. G is predicted by theory to be linearly proportional to the polymer number density (Bird et al., 1987), which in the present context is in turn linearly proportional to matrix density. Thus, a linear relationship between τ_{wg} and G would imply a linear relationship between τ_{wg} and matrix density.

At any given instant, biofilm structural and mechanical response appears to be dominated by the EPS-cell matrix. This matrix, as well as the material properties noted above, can be well described by what has been called an associated polymer system (Leiber et al., 1991; Rubinstein and Dobrynin 1997)—a polymeric material consisting of polymers that form weak interlinking bonds that break and reform on laboratory time-scales (say 10's of sec, written $O(10^1 \text{s})$), for example, systems of intermolecular bonds (e.g., hydrogen bonds), as opposed to stronger ionic or covalent bonds. Intermolecular bonds result in an elastic polymer matrix; however, if the bonding is weak, under stress the matrix can deform irreversibly on the time scale of bond breakage
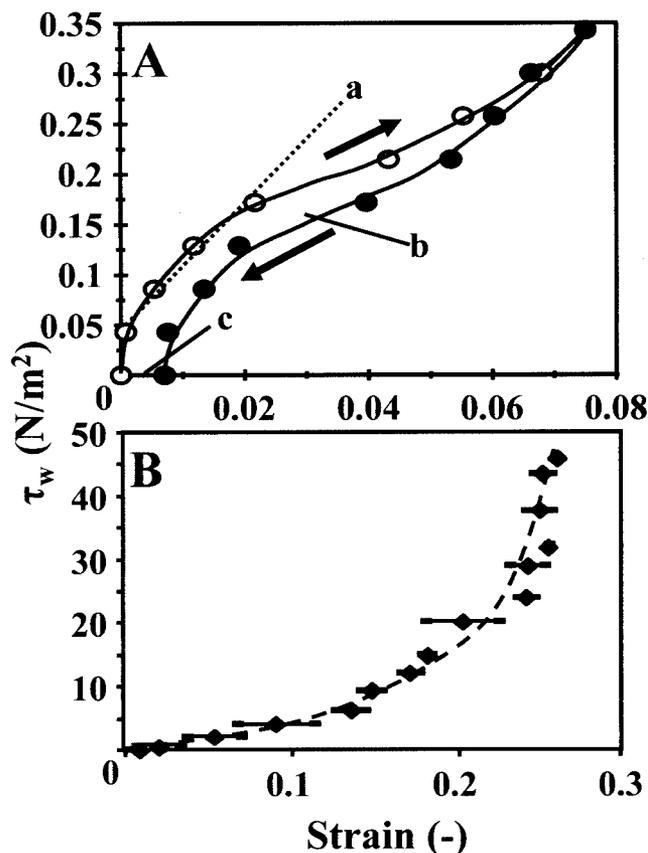

Figure 3. Stress–strain curves for the mucoid strain *P. aeruginosa* FRD1. The biofilm was grown at a flow velocity of 0.004 m/s, $\tau_{wg} = 0.007$ N/m². A: Low stress test curve was sigmoidal. Loading and unloading portions of the test are indicated by the "up" and "down" arrows, respectively. The G of the low modulus linear region "a" was approximately 6 N/m². Hysteresis between the loading and unloading portions of the test "b" and the residual strain "c" are characteristic of a viscoelastic fluid. B: High shear test on the same biofilm showed a J-shape curve, characteristic of biological materials such as rubber or collagen. The biofilm became progressively stiffer at higher strains.

and reformation throughout the matrix. Hence, viscous flow may also be observed over longer time scales. Note that the elastic strength and also the flow time scale and resulting viscosity depend on the bonding density.

We briefly describe the EPS-cell matrix and its stress response as follows: in the absence of external stress, the

Table II. The measured apparent elastic modulus (G) of *P. aeruginosa* grown at different wall shear stresses (τ_{wg}).

τ_{wg} (N/m²)	G (N/m²)	Strain	Reference
0.005	0.87 ± 0.18, n=6	JP1	This study
0.007	2.78 ± 0.1, n=2	FRD1	This study
0.09	26.5 ± 6.3, n=3	PAO1	Stoodley et al. (2001b)
5.1	64.67 ± 21.03, n=6	PAO1	This study
5.3	99.60 ± 66.10, n=6	PAO1	Stoodley et al. (2001b)

n refers to replicate measurements made in different microcolonies in the biofilm.
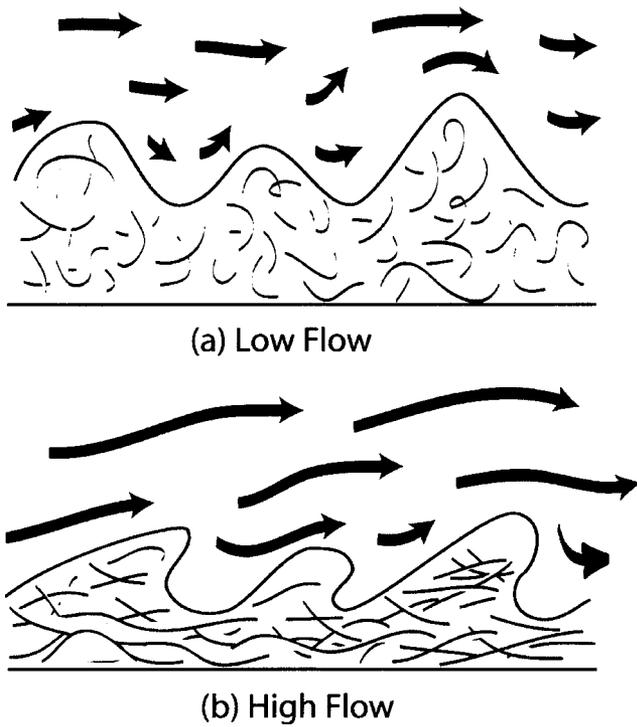
Figure 4. Stress–strain response experiment: (A) pure elastic response, (B) elastic deformation and recoil with hysteresis, i.e., irreversible viscous flow.

matrix relaxes to an isotropic polymeric tangle with density determined by a balance between attractive hydrogen bonding (and possibly entanglement forces) vs. repulsive excluded volume and entropic forces. Consider now applying an external stress to the biofilm through bulk fluid flow (Fig. 4). The EPS matrix responds to stress by exhibiting 1) elastic tension due to a combination of polymer entanglement, entropic, and weak hydrogen bonding forces; 2) viscous damping due to polymeric friction and hydrogen bond breakage; and 3) alignment of polymers in the shear direction.

Breakage of hydrogen bonds also allows the biofilm to exhibit creep (Fig. 3a), although possibly very slowly if the polymer viscosity is high. Another consequence of polymer alignment is a reduction of exclusionary entropic forces between polymers. Coupled with hydrogen bond interaction, we would then expect to see polymer attraction and hence an increase in the dry EPS-cell matrix density. Such behavior would result in a loss of biofilm volume through water extrusion and an increase in biofilm elastic modulus G due to increased EPS concentration. In addition, a less tangled EPS matrix allows better interlinking between EPS strands so that the elastic relaxation time λ (the characteristic time for internal elastic stress relaxation) should increase.

Subsequent removal of external stress will result in response to property (1) in an elastic recoil of the biofilm over the elastic response time and, in response to property (3), in a relatively slow relaxation of polymer

conformation back to its isotropic tangled state, including reduction of dry density and reexpansion of volume. We then expect biofilm matrix elastic and viscous material properties to return to their unstressed values on the longer time scale.

The ionic environment may also significantly effect biofilm material properties. Crosslinking agents such as Ca^{++} or Al^{+++} can replace week hydrogen bonds with strong ionic crosslinks in the EPS matrix (Stoodley et al., 2001a; Koerstgens et al., 2001). These studies indicate that the EPS-cell matrix has formed something more like a strong gel than an associated system. The result is a considerably stronger elastic solid without noticeable viscous flow, a confirmation of the proposed associated polymer model at low crosslinking agent concentrations.

Biofilm Model Equations

The biofilm evolution equations are then as follows: defining $\mathbf{u}$ to be the biofilm matrix velocity field and ρ to be the biofilm matrix density, the standard fluid equations take the form:

$$(\rho\mathbf{u})_t + \nabla \cdot (\rho\mathbf{u} \otimes \mathbf{u}) = \nabla \cdot \sigma \qquad (1)$$

$$\rho_t + \nabla \cdot (\rho\mathbf{u}) = g \qquad (2)$$

where σ is the biofilm matrix stress tensor to be described below and g is a biofilm matrix growth source (or sink) term. The subscript t signifies time differentiation.

Frequently, we consider phenomena evolving quasistatically so that time derivatives can be neglected. On the other hand, the time scales of interest here are much shorter than the biofilm growth time so that g can also be neglected. Additionally, the inertial term can typically be neglected due to large viscosity of the biofilm. Altogether, then, [1] and [2] simplify to:

$$\nabla \cdot \sigma = 0 \qquad (3)$$

$$\nabla \cdot (\rho\mathbf{u}) = 0 \qquad (4)$$

Stress–Strain Law

The stress tensor σ determines the response of the biofilm to deformation through a stress–strain law. Knowledge of the appropriate stress–strain relation is essential for understanding and prediction of stress distribution through the biofilm and, hence, important observed properties such as sloughing. We propose here a stress–strain law based on the biofilm material physics described above. σ can be broken into two pieces:

$$\sigma = \sigma_P + \sigma_d, \qquad (5)$$

the pressure stress σ_p and the so-called deviatoric stress σ_d. For σ_d we utilize a linear Jeffreys constitutive law (Joseph, 1990):

$$(\sigma_d)_t + \sigma_d/\tau = G(\mathbf{D} + \Lambda \mathbf{D}_t) \qquad (6)$$

where:

$$\mathbf{D} = 1/2(\nabla \mathbf{u} + \nabla \mathbf{u}^T) \qquad (7)$$

is the fluid rate-of-strain matrix and τ and G are the elastic relaxation time and elastic modulus, respectively. The retardation time Λ is a measure of viscous delay of elastic deformation on short time scales. In particular, for motions on time scales short compared to λ, a Jeffreys material acts like a viscoelastic solid (σ_d/λ in [6] can be neglected); for motions on time scales long compared to λ it acts like a viscous fluid (time derivatives in [6] can be neglected). By choosing a linear constitutive law we implicitly assume a slow biofilm deformation rate, a restriction consistent with slow biofilm motion. For modeling rapid deformations, nonlinear modifications are necessary. For example, the Jeffreys stress–strain law [6] will not exhibit J-shaped stress–strain curves. Restriction to slow deformations is, however, a useful first step and pending more material property data a reasonable one.

In fact, we do include a slow nonlinearity to account for the biofilm's shear thickening in response to environmental stress as follows: we suppose $\lambda = \lambda(\rho)$ is an increasing function of ρ, i.e., the denser the EPS, the longer the viscous relaxation. We also suppose that $G = G(\rho)$ is an increasing function of ρ, i.e., the denser the EPS, the stronger the elastic response. In principle, biofilm elastic response need not be isotropic, in which case G should be a tensor; however, for simplicity we will presume G to be a scalar. As previously mentioned, standard molecular theory predicts $G(\rho) = C_g \rho^{\kappa 1}$ for some constants C_g and $\kappa 1$ with, in many polymeric materials, $\kappa 1 = 1$ (Bird et al., 1987). We also choose $\lambda(\rho) = C_\lambda \rho^{\kappa 2}$ for some constants C_λ and $\kappa 2$, again under the assumption that opportunity for hydrogen bonding scales with EPS density. Note that in the case of system time scales considerably longer than the elastic relaxation time λ, we can set time derivatives to zero so that:

$$\sigma_d = \lambda G \mathbf{D} = C \rho^{\kappa 1 + \kappa 2} \mathbf{D} = 2\eta \mathbf{D} \qquad (8)$$

where η is a fluid viscosity.

The second part of the stress tensor, the pressure stress, is an isotropic tensor of the form $\sigma_p = -p\mathbf{I}$ with assumed constitutive law:

$$p = c^2(\rho - \rho_0(\sigma_d)) \qquad (9)$$

where ρ_0 is the preferred biofilm matrix density at a given deviatoric stress σ_d and c is a density relaxation wave speed. The form of [9] is chosen to be essentially as

simple as reasonable pending more data. More generally, a power law relationship might be assumed. For sufficiently slow change, we can assume $\rho = \rho_0$. The constitutive function $\rho_0(\sigma_d)$ is assumed to be of the form:

$$\rho_0(\sigma_d) = \alpha\sqrt{\mathrm{Tr}(\sigma_d^2)} + \beta \qquad (10)$$

where $\rho_0(0) = \beta$ is the unstressed preferred EPS density and α is a proportionality constant. Here, for a given matrix $\mathbf{M}$, $\mathrm{Tr}(\mathbf{M})$ is the trace of $\mathbf{M}$, i.e., the sum of the diagonal elements of $\mathbf{M}$. $\mathrm{Tr}(\sigma_d^2)$ is the sum of squares of the principle stresses, providing a measure of the total local stress (squared). The linear relationship in [10] is, as previously mentioned, a consequence of the presumed linear relationship between τ_{wg} and G.

In addition to the biofilm matrix tension, there is also a hydrostatic pressure. This pressure, however, can be assumed to be constant throughout the biofilm layer due to the thinness of the layer, typically on the order of 10^2 μm.

Estimation of Parameters

Data on biofilm material properties are limited at the current time, although we expect this situation to be remedied with future studies. For the moment, however, we are restricted to order of magnitude estimates of material parameters. However, we believe that proposing a constitutive model based on the best available data is a useful step, first to provide rough estimates of model parameters, and second to check consistency of available data with the proposed model. It should also be noted that material parameters can be expected to vary between species due to differences in EPS.

We begin with the two parameters α and β contained in expression [10] for the stressed equilibrium density $\rho_0(\sigma_d)$. Rough estimates for these quantities can be obtained using data of Vieira et al. (1993) of biofilms grown at two different Reynolds numbers. In a flat layer geometry, $\sqrt{\mathrm{Tr}(\sigma_d^2)}$ reduces to the horizontal shear stress. Under that assumption, averaging of their density vs. τ_{wg} values finds $\alpha = 14$, $\beta = 7$ (in mks units).

The density wave speed c^2 in the constitutive law [9] can be estimated from the approximate density relaxation time of $O(10^3 \mathrm{s})$ required for a biofilm streamer to relax after a change in fluid stress. This can be observed, for example, in Stoodley et al. (1999a, Fig. 9), where it is apparent that the biofilm viscosity has changed by a factor of about 2.5 after stressing or unstressing time periods of order $t = 60$ min, plausible in response to increased average fluid shear stress over the $t = 30$ to $t = 90$ time period. Estimating a biofilm streamer thickness at 10^{-5}m (see e.g., Fig. 1), we find that $c \approx d/t \approx O(10^{-8} \mathrm{m/s})$.

We can use data from flow cell experiments to estimate the viscoelastic parameters G and λ. Stoodley et al.

Table III. Biofilm viscosity (η) and relaxation time (λ) estimated from the flow velocity and morphology of biofilm ripples measured at different wall shear stresses (τ_w).

τ_w (N/m^2)	Ripple velocity (μm/h)	Biofilm thickness (μm)	Calculated viscosity (Ns/m^2)	λ (s)
0.73	480	48	2.7E + 02	15.65
1.5	900	28	1.3E $\pm$ 2	4.57
2.5	290	14	4.3E + 02	9.94
3.7	100	12	1.6E + 03	26.17
5.1	32	14	8.0E + 03	97.31
6.7	30	22	1.8E + 04	169.5

Data was taken from Stoodely et al. (1999b). Viscosity was calculated from the shear rate which was estimated from the thickness of the biofilm and the velocity of the ripples at the biofilm/bulk liquid interface. $\tau_{wg} = 5.09$ N/m^2

(2001b) measured the elastic modulus G at a number of different bulk flow rates by tracking deformation of biofilm topography under shear stress perturbations (Table II). Setting $G = C_G\rho^{\kappa 1}$ and using [10] with parameters set to $\alpha = 14$, $\beta = 7$ to estimate ρ, we obtain nonlinear least-squares fits of $C_G = 0.92$ and $\kappa_1 = 1.03$. Note molecular theory predicts $\kappa 1 = 1$. However, the centered 95% confidence intervals for C_G and $\kappa 1$ are [−1.79, 3.63] and [0.35, 1.70], respectively, even assuming the values of α and β are exactly correct. Thus, the data here are consistent with the proposed model but are not conclusive.

A number of experiments have used a flow cell setup consisting of a horizontal stress of magnitude Σ imposed on the top boundary of a biofilm layer. Under this geometry the viscoelastic fluid equations have steady solution $\mathbf{u}(x,z) = (\mathbf{u}(z),0)$ with:

$$\rho = \alpha\Sigma + \beta \qquad (11)$$

$$\mathbf{u}(z) = (2\Sigma/\lambda G)z \qquad (12)$$

and $\rho = \rho_0(\sigma_d)$. Note again that the product λG takes the form of a viscosity.

To obtain an estimated biofilm viscosity η at varying shear stresses, we use [12] and data from biofilm ripple observations (Stoodley et al., 1999b). Setting $\lambda G = C_\lambda C_G\rho^{\kappa 1 + \kappa 2}$ with C_G, $\kappa 1$ as above we obtain nonlinear least-square fits of $C_\lambda = 0.0004$, $\kappa 2 = 2.82$. $\kappa 2 \geq 1$, as expected for polymeric systems (Bird et al., 1986) but, again, note that the centered 95% confidence intervals for C_λ and $\kappa 2$ are [−0.0015, 0.0022] and [1.74, 3.91], respectively. We find a relaxation time at higher shear stresses of $\lambda = O(10^2 \text{s})$, consistent with observations and hence providing another confirmation of the theory.

We roughly estimate the elastic retardation time Λ using loss modulus data from dynamic testing of intact *P. aeruginosa* biofilms grown at $\tau_{wg} = 5$ N/m^2 on the place of a cone and plate Weissenberg rheometer (Characklis 1980). Elastic modulus estimates for those biofilms are unavailable. However, estimating $G = O(10)$ as in Table II and combining with the Characklis loss modulus data results in $\Lambda \equiv 10$ s.

Final Remarks

Conceptually, one may ask the following question: How should a biofilm respond to external mechanical stress to best maintain structural integrity? In the laboratory, biofilms apparently respond with a combination of elastic tension on short time scales and viscous flow on long time scales. The balance of elastic strength vs. viscous relaxation and the crossover time from one to the other depends in part on the biofilm history. Higher stress results in stronger elasticity and longer elastic relaxation times. All of this seems sensible—short, sharp perturbations are absorbed elastically but if external stress is maintained for too long a pure elastic response risks material failure. Hence, the biofilm dissipates the induced stress through viscous flow. If the external perturbation persists over even longer times the biofilm resists excess flow displacement by both stiffening elastically and increasing viscous dissipation through contraction.

CONCLUSIONS

Based on biofilm creep data we conclude that biofilms behave as viscoelastic fluids, demonstrating both unreversed flow as well as elastic and viscoelastic recoil. Data also point to the possibility of modeling biofilms as associated polymer systems with an elastic relaxation time on the order of minutes and mechanical contraction in response to shear stress. Use of a Jeffreys viscoelastic fluid constitutive law together with shear responsive tension qualitatively matches observed biofilm mechanical behavior.

NOMENCLATURE

c	density relaxation wave velocity	(m/s)
C_G	elastic modulus coefficient	(kg$^{1-\kappa 1}$/m$^{1-3\kappa 1}$s^2)

C_λ	elastic relaxation time coefficient	$(m^{3\kappa2}\, s/kg^{\kappa2})$
D	rate-of-strain matrix	(1/s)
g	biofilm growth source	$(kg/m^3 \cdot s)$
G	elastic modulus	$(kg/m \cdot s^2)$
u	biofilm matrix velocity	(m/s)
p	stress-induced pressure	$(kg/m \cdot s^2)$
α	stress-density coupling modulus	s^2/m^3
ϵ	strain	
$\kappa1, \kappa2$	unitless scaling exponents	
λ	elastic relaxation time	(s)
Λ	elastic retardation time	(s)
ρ	dry biofilm density	(kg/m^3)
ρ_0	preferred dry biofilm density	(kg/m^3)
β	zero stress dry biofilm density	(kg/m^3)
σ	biofilm stress tensor	$(kg/m \cdot s^2)$
σ_p	biofilm pressure stress tensor	$(kg/m \cdot s^2)$
σ_d	biofilm deviatoric stress tensor	$(kg/m \cdot s^2)$
Σ	external shear stress	(N/m^2)
τ_w	wall shear stress	(N/m^2)
τ_{wg}	specific wall shear stress during growth	(N/m^2)
η	biofilm viscosity	$(kg/m \cdot s)$

References

Bird RB, Curtiss CF, Armstrong CA, Hassager O. 1987. Dynamics of polymeric liquids, vol. 2. Kinetic theory. New York: John Wiley & Sons.

Characklis WG. 1980. Biofilm development and destruction. Electric Power Research Institute Final Report. Palo Alta, CA: EPRI CS-1554, RP902-1.

Dillon R, Fauci L, Fogelson A, Gaver D. 1996. Modeling biofilm processes using the immersed boundary method. J Comp Phys 129:57–73.

Dockery J, Klapper I. 2001. Finger formation in biofilm layers. SIAM J Appl Math 62:853–869.

Flemming HC, Wingender J, Mayer C, Koerstgens V, Borchard W. 2000. Cohesiveness in biofilm matrix polymers. In: Allison D, Gilbert P, Lappin-Scott HM, Wilson M, editors. Community structure and cooperation in biofilms. Cambridge: SGM Symposium Series 59, Cambridge University Press. p 87–105.

Gujer W, Wanner O. 1990. Modeling mixed population biofilms. In: Characklis WG, Marshall KC, editors. Biofilms. New York: John Wiley & Sons. p 397–443.

Hermanowicz WS. 1998. Two-dimensional simulations of biofilm development: effects of external environmental conditions. In: Rittmann BE, Bishop P, Bouwer E, Cunningham A, editors. Conference proceedings, international specialty conference. Microbial ecology of biofilms: concepts, tools and applications. Lake Bluff, IL:.

Holloway BW, Kirshnapillai V, Morgan AF. 1979. Chromosomal genetics of Pseudomonas. Microbiol Rev 43:73–102.

Joseph DD. 1990. Fluid dynamics of viscoelastic liquids. New York: Springer-Verlag.

Koerstgens V, Flemming H-C, Wingender J, Borchard W. 2001. Influence of calcium ions on the mechanical properties of a model biofilm of mucoid *Pseudomonas aeruginosa*. Water Sci Technol 43:49–57.

Leiber L, Rubinstein M, Colby RH. 1991. Dynamics of reversible networks. Macromolecules 24:4701–4707.

Nivens DE, Ohman DE, Williams J, Franklin MJ. 2001. Role of alginate and alginate o-acetylation in the formation of *Pseudomonas aeruginosa* microcolonies and biofilms. J Bacteriol 183:1047–1057.

Ohashi A, Harada H. 1994. Adhesion strength of biofilm developed in an attached-growth reactor. Water Sci Technol 29:281–288.

Pearson JP, Pesci EC, Iglewski BH. 1997. Roles of *Pseudomonas aeruginosa las* and *rhl* quorum-sensing systems in control of elastase and rhamnolipid biosynthesis genes. J Bacteriol 179:5756–5767.

Picioreanu C, van Loosdrecht MC, Heijnen JJ. 2001. Two-dimensional model of biofilm detachment caused by internal stress from liquid flow. Biotechnol Bioeng 72:205–218.

Piriou P, Dukan S, Levi Y, Jarrige PA. 1997. Prevention of bacterial growth in drinking water distribution systems. Water Sci Technol 35:283–287.

Rubinstein M, Dobrynin AV. 1997. Solutions of associative polymers. Trends Polym Sci 5:181–186.

Stoodley P, Lewandowski Z, Boyle J, Lappin-Scott HM. 1998. Oscillation characteristics of biofilm streamers in flowing water as related to drag and pressure drop. Biotechnol Bioeng 57:536–544.

Stoodley P, Lewandowski Z, Boyle JD, Lappin-Scott HM. 1999a. Structural deformation of bacterial biofilms caused by short term fluctuations in flow velocity: an in-situ demonstration of biofilm viscoelasticity. Biotechnol Bioeng 65:83–92.

Stoodley P, Lewandowski Z, Boyle JD, Lappin-Scott HM. 1999b. The formation of migratory ripples in a mixed species bacterial biofilm growing in turbulent flow. Environ Microbiol 1:447–457.

Stoodley P, Jacobsen A, Dunsmore BC, Purevdorj B, Wilson S, Lappin-Scott HM, Costerton JW. 2001a. The influence of fluid shear and AlCl3 on the material properties of *Pseudomonas aeruginosa* PAO1 and *Desulfovibrio sp.* EX265 biofilms. Water Sci Technol 43:113–120.

Stoodley P, Hall-Stoodley L, Lappin-Scott HM. 2001b. Detachment, surface migration and other dynamic behavior in bacterial biofilms revealed by digital time-lapse imaging. Methods Enzymol 337:306–319.

Vieira MJ, Melo LF, Pinheiro MM. 1993. Biofilm formation: hydrodynamic effects on internal diffusion and structure. Biofouling 7:67–80.

Vincent J. 1990. Structural biomaterials. Lawrenceville, NJ: Princeton University Press.

Walker JT, Mackerness CW, Mallon D, Makin T, Williets T, Keevil CW. 1995. Control of legionella-pneumophila in a hospital water-system by chlorine dioxide. J Indust Microbiol 15:384–390.

Zottola EA, Sasahara KC. 1994. Microbial biofilms in the food industry — should they be a concern? Int J Food Microbiol 23:125–148.